

Rensselaer Polytechnic Institute
Troy, New York

Annual Report
Contract No. EY-76-S-02-3459.*000

EFFECTS OF HYDROGEN ON FATIGUE OF VANADIUM AND NIOBIUM

January 15, 1977

Prepared by
Norman S. Stoloff
Professor of Materials Engineering

and

D. W. Chung
Research Associate in Materials Engineering

MASTER

NOTICE
This report was prepared as an account of work sponsored by the United States Government. Neither the United States nor the United States Energy Research and Development Administration, nor any of their employees, nor any of their contractors, subcontractors, or their employees, makes any warranty, express or implied, or assumes any legal liability or responsibility for the accuracy, completeness or usefulness of any information, apparatus, product or process disclosed, or represents that its use would not infringe privately owned rights.

This report was prepared as an account of work sponsored by the United States Government. Neither the United States nor the United States Energy Research and Development Administration, nor any of their employees, nor any of their contractors, subcontractors, or their employees, makes any warranty, express or implied, or assumes any legal liability or responsibility for the accuracy, completeness, or usefulness of any information, apparatus, product or process disclosed or represents that its use would not infringe privately owned rights.

DISCLAIMER

This report was prepared as an account of work sponsored by an agency of the United States Government. Neither the United States Government nor any agency Thereof, nor any of their employees, makes any warranty, express or implied, or assumes any legal liability or responsibility for the accuracy, completeness, or usefulness of any information, apparatus, product, or process disclosed, or represents that its use would not infringe privately owned rights. Reference herein to any specific commercial product, process, or service by trade name, trademark, manufacturer, or otherwise does not necessarily constitute or imply its endorsement, recommendation, or favoring by the United States Government or any agency thereof. The views and opinions of authors expressed herein do not necessarily state or reflect those of the United States Government or any agency thereof.

DISCLAIMER

Portions of this document may be illegible in electronic image products. Images are produced from the best available original document.

ABSTRACT

The fatigue behavior of unalloyed vanadium and niobium as well as their alloys with hydrogen is described. The response of vanadium-hydrogen alloys to cyclic loading is shown to depend markedly upon the presence or absence of notches, the hydrogen level, method of test, and frequency. In general, hydrides improve high cycle life of unnotched alloys, but are detrimental in the presence of a notch. Low test frequencies also lead to reduced fatigue lives. Stress-assisted hydride growth in previously hydrided alloys has been noted both in fatigue and in delayed failure experiments. Unalloyed vanadium and solid solution vanadium-hydrogen alloys do not undergo delayed failure.

Preliminary tests on unalloyed niobium and several niobium-vanadium alloys reveal improvements in stress-controlled fatigue life and decreased low cycle life, in agreement with previous observations on vanadium-hydrogen alloys.

BACKGROUND

We have previously reported significant improvements in the unnotched high cycle (stress control, test frequency > 10 Hz) fatigue life of polycrystalline vanadium when hydrogen in excess of the solubility limit is added. However, under low cycle conditions (strain control, test frequency < 1 Hz) hydrides are detrimental to fatigue resistance. In an effort to determine the causes of the pronounced differences in response to the two test methods, we have conducted a test program involving the following features:

1) Study of crack initiation times and crack propagation rates as a function of hydrogen content in notched sheet.

2) Determination of high cycle fatigue properties of notched $V-H_2$ bars.

3) Study of stress-induced hydride formation by means of delayed failure experiments.

4) Determination of frequency effects on high cycle fatigue of $V-H_2$ alloys.

In addition, a study of the effects of hydrogen on fatigue properties of unnotched Nb has commenced. In view of the great amount of information obtained in the past year, this report is divided into four distinct sections:

Part 1: Effects of Hydrogen on Fatigue Crack Initiation and Propagation in Vanadium

Part 2: Delayed Failure and Fatigue Notch Sensitivity of $V-H_2$ Alloys

Part 3: Effects of Test Frequency on Fatigue of $V-H_2$ Alloys

Part 4: Fatigue of Niobium-Hydrogen Alloys

A general summary of the status of the various test programs appears at the end of the report.

Part 1

EFFECTS OF HYDROGEN ON FATIGUE CRACK PROPAGATION IN VANADIUM

INTRODUCTION

The effects of hydrogen on monotonic mechanical behavior of the group Va refractory metals: Ta, V and Nb have been extensively investigated. Strengthening by the presence of hydrogen in solution and hydride precipitates in these metals appears to occur within certain range of temperatures, but reduced ductility (hydrogen embrittlement) at low temperature also has been observed.¹⁻³ Little attention, however, has been directed to the influence of hydrogen on cyclic deformation and fatigue crack propagation in the refractory metals.

Wilcox⁴ showed that hydrogen in solution (as well as in the form of hydrides) significantly reduced the fatigue life of tantalum and thus concluded that hydrogen embrittlement was associated with an increased ease of both crack initiation and crack propagation. In contrast, Lee and Stoloff⁵ recently reported significant improvements in high cycle (stress-controlled) fatigue life when hydrogen was introduced into vanadium as hydrides. Those tests were conducted in tension-compression. Furthermore, fatigue lives of hydrided vanadium were several times longer than for an alloy with 132 ppm hydrogen in solution at a similar stress level.

The present investigation extends the work of Lee and Stoloff⁵ to take into account the separate effects of various levels of hydrogen on time for crack initiation and crack propagation rates in vanadium.

Various stress ranges and mean stresses have been applied in stress-controlled tests at room temperature. Fatigue crack growth characteristics also have been compared with tensile properties. Fracture mode were observed by means of metallography and scanning electron microscopy.

EXPERIMENTAL PROCEDURE

Vanadium was received from Wah Chang Corporation in the form of annealed sheet with a grain size $\sim 50 \mu\text{m}$. Fatigue specimens of single-edge notch type were machined from the original material. Following mechanical polishing up to $6 \mu\text{m}$ diamond compound, electrolytic polishing was conducted in $\text{H}_2\text{SO}_4\text{-H}_2\text{O}$ solution, applying 30 volts at 0°C . All samples were then annealed for 2 hours at 760°C in vacuum of 10^{-7} torr to obtain a final grain size of $\sim 80 \mu\text{m}$. Hydrogen was added as described previously.⁵ The chemical analyses of vanadium and the vanadium alloys, as well as the size of hydrides, are listed in Table 1. The microstructures of the hydrogen-charged vanadium were similar to those reported in ref. 5.

Fatigue tests were conducted at room temperature as previously described,⁵ using a sinusodial loading cycle at a cyclic frequency of 20 Hz. During the fatigue tests measurements of crack length were made by means of replicating thin plastic tape at the fracture surface; accuracy was estimated to be 2×10^{-4} cm. The tests were terminated when the crack had reached a length of 60% of specimen width. The stress intensity range, ΔK , was determined from a K calibration with the following expression:⁶

$$\Delta K = \Delta\sigma\sqrt{a} f(a/w) \quad (1)$$

where $f(a/w) = 1.99 - 0.41(a/w) + 18.70(a/w)^2 - 38.48(a/w)^3 + 53.85(a/w)^4$
 with $\Delta\sigma$ the gross applied stress, a the effective half crack length and w the specimen width.

RESULTS

Fatigue Crack Propagation

Crack growth rates, da/dN , are presented in the form of log-log plots of da/dN versus ΔK :

$$da/dN = C(\Delta K)^m \quad (2)$$

as described by Paris and Erdogan.^{7,8}

Fig. 1 shows data plotted for annealed vanadium and the hydrogen charged vanadium at a stress ratio ($\sigma_{min}/\sigma_{max}$) = 0.4. It shows that the crack growth rates for a given ΔK were essentially similar in annealed vanadium and the 200 ppm H_2 alloy although the yield stress of the 200 ppm H_2 vanadium was significantly higher than that of annealed vanadium.⁵ In contrast to the low hydrogen alloys, the crack growth rates of the high hydrogen alloys deviate significantly from linearity; however, we will continue to use Eq. 2 as a basis for discussion. Increasing hydrogen content in solution to 420 ppm seems to increase the slope of da/dN vs. ΔK , but for a given ΔK the crack growth rate in the two phase 1500 ppm H_2 vanadium was much lower than that of the 420 ppm H_2 alloy. Fig. 2 shows data for the stress ratio $R = 0.05$, for the high hydrogen alloys. Linear plots were obtained for 420 and 845 ppm alloys only. The irregular behavior at higher hydrogen contents seems to be associated with the shape and the amount of the hydride precipitates. The crack growth rate of the 845 ppm H_2 alloy for a given ΔK was the lowest among the hydrided alloys. Detailed examination of the crack surface on this alloy clearly showed stress induced hydrides at the crack tip; the redistribution of hydrogen by stress resulted in the growth of large hydrides, as will be shown below.

The low value of the crack growth rate in the 845 ppm H₂ vanadium also may be related to different fracture morphologies among the hydrided alloys.

Certain features of the rate curves for the higher mean stress values are different from that for the low mean stress value. In the low hydrogen (200 ppm) alloy an increase in the mean stress significantly increases the crack growth rate and this is consistent with results for brittle materials.⁹ In the 1500 ppm H₂ alloy, on the other hand, the crack growth rate was little influenced by the stress ratio over the entire range of ΔK. With regard to the crack growth rate of the hydrided vanadium, there is generally a slope transition for all the stress ratios, similar to that of aluminum alloys containing inclusions.¹⁰ This result is consistent with observations of stress-assisted hydride growth during cyclic loading.

Information on fatigue crack nucleation in vanadium and the hydrogen charged vanadium alloys was obtained by determining the number of cycles to initiate a crack in the notched samples. Fig. 3 indicates a relative merit of the hydrided alloys in delaying crack initiation, while little influence of low hydrogen content (200 ppm) was observed.

Metallography

In order to study the formation of stress induced hydrides, the 420 ppm and 845 ppm H₂ alloys were chosen for observation of the fatigued surface during crack propagation. A series of replicas at the crack tips, investigated for the 845 ppm H₂ vanadium alloy, showed several new hydride particles which had not been seen when the crack tip was far away from it. Also noted was the dissolution of a hydride simultaneous with the growth of the adjacent hydride.

It should be noted that since crack initiation at interfaces of hydrides has not been observed, the hydride particles in vanadium do

not seem to aid crack initiation; rather they behave as obstacles during crack propagation. Micrographs of the crack propagation surface in the 420 ppm alloy failed to reveal formation of any stress-assisted hydrides at the crack tip.

Fractographic Observations

The fracture surface in annealed vanadium revealed ductile striations, as previously reported for unnotched specimens.⁵ The presence of a small amount of hydrogen in solution (200 ppm) had no effect on fractographic features. However, the 420 ppm H₂ alloy (near the solubility limit at room temperature, 460 ppm) revealed cleavage facets. Brittle cleavage was observed also in the 1500 ppm H₂ alloy. The general features of the fracture surfaces in the present alloys are consistent with those reported in the previous work.⁵

DISCUSSION

The fatigue crack propagation parameters in Eq. 2 for vanadium and vanadium alloys at various stress ranges and mean stress ratios are listed in Table 2. It can be seen that the power law exponent, m , at a stress ratio of $R = 0.4$, noticeably increases, from 2.67 to 6.99, with hydrogen concentration in solution in vanadium, but in the hydrided vanadium, the m value increases further only to 7.7. A comparison between the 420 ppm vanadium (hydrogen in solution) and the 1500 ppm vanadium (hydrided) alloys by varying the mean stress ratio shows that m values in 420 ppm vanadium increase with R , while in 1500 ppm vanadium no significant increment occurs, apart from the result at $R = 0.516$.

The effect of hydrogen on fatigue crack growth rates should be relatable to some combination of properties such as yield strength, σ_y ,

and fatigue strain hardening exponent, n' , which will eventually control the size and properties of the plastic zone at the crack tip. An inverse relationship between m and n' has, in fact, been reported in the literature.^{11,12}

Several attempts have been made to derive the fatigue crack growth equation related to the mechanical property parameters, but the only model which takes into account directly the fatigue strain hardening characteristic of materials is that proposed by Tomkins.¹³

In terms of the stress intensity factor range ($\Delta K = \Delta \sigma \sqrt{a}$):

$$\frac{da}{dN} = A \frac{\Delta K^{(1+n')/n'} \sigma_m}{(2k)^{1/n'} (\sigma_y)^2 (a)^{(1-n')/2n'}} \quad (3)$$

$$A = \frac{\pi^2}{32}$$

$$k = \sigma_a / \left(\frac{\Delta \epsilon_p}{2} \right)^{n'} \quad (\text{obtained from a cyclic stress-strain curve})$$

For most of the experimental conditions of this work, $0.2 < a/w < 0.5$ where w is specimen width, and thus for a constant w , $K^{1/n'}$, $a^{(1-n')/2n'}$ and σ_m should be relatively constant.

Therefore, Eq. 3 further reduces to a simple form of crack growth law:

$$\frac{da}{dN} = C \frac{\Delta K^{1/n'+1}}{(\sigma_y)^2} \quad (4)$$

where C is a constant.

Comparison of the present growth rate data with the fatigue strain hardening results reported previously⁵ for the various hydrogenated vanadium alloys, Table 3, shows a strong inverse relation between m and n' values in both unalloyed and hydrogen-charged alloys. To obtain a proportionality factor, called m' , the m value was set equal to m'/n' . As a result two distinct regions of m' values between low and high hydrogen vanadium alloys were evaluated to be $m' = 0.931$ and $m' = 0.665$ respectively. This may be rather fortuitous since n' values in two hydrided alloys, as indicated in Table 3, are uncertain but the results seem to be within the limits between two extreme values, one each for low and high hydrogen alloys. Consequently, the present results for the power law exponent could be explained in terms of the fatigue strain hardening coefficient with a relationship of $m = 0.931/n'$ for hydrogen in solution and $m = 0.665/n'$ for the hydrided vanadium alloys.

A simple relation also has been observed between the crack growth rate constant, C , and yield stress, σ_y , as shown in Table 4. The growth rate constants for each alloy decrease with increases in m and hydrogen concentration in alloys, which agrees with various models suggested in the literature.¹⁴⁻¹⁶ It has been suggested¹⁴ that the fatigue crack growth rate should be related to the crack opening displacement, which is inversely proportional to the square of yield strength, σ_y^2 . In the present work, Table 4 shows a relationship between the constant, C , in the growth equation and σ_y . By setting $C = \alpha/\sigma_y^2$, where α is a structural constant, two regions of α values between low and high hydrogen alloys were found: $\alpha = 6.4 \times 10^{-7}$ and $\alpha = 1.4 \times 10^{-8}$, respectively. Thus the results in the vanadium alloys for all test conditions may be represented in two different forms of the crack growth equation; namely, for hydrogen

in solution:

$$\frac{da}{dN} = 6.4 \times 10^{-7} \frac{\Delta K^{0.931/n'}}{\sigma_y^2} \quad (5)$$

For the hydrided vanadium alloys:

$$\frac{da}{dN} = 1.387 \times 10^{-8} \frac{\Delta K^{0.665/n'}}{\sigma_y^2} \quad (6)$$

Cracking in all alloys was generally transgranular although intergranular cracking was occasionally observed. In both types of alloy (hydrogen in solution and hydrides) the nucleation and initial propagation of cracks was commonly at a single location; multiple cracking was often seen only at the end of the fracture process, when unstable fracture occurred at higher stresses. The absence of secondary cracks in hydrided vanadium also indicates that cleavage of the pre-existing hydride was not the primary fracture mechanism. In-situ studies of fatigue crack propagation, and an analysis of stresses at the crack tip both suggest the growth of stress-induced hydrides, but only in the previously hydrided alloys.

Part 2

DELAYED FAILURE AND FATIGUE NOTCH SENSITIVITY
OF VANADIUM-HYDROGEN ALLOYSINTRODUCTION

Studies on the mechanical properties of the group Va refractory metals: Ta, V and Nb, have revealed hydrogen embrittlement characteristics at low temperatures,¹⁻³ but there has been little or no work reported on delayed failure. It might be anticipated in these materials that the high mobility of hydrogen at room temperature would enhance migration to the region of stress concentration (notch root) and affect time-dependent fracture behavior. In ref. 5 and Part 1 of this report are described fatigue experiments on vanadium-hydrogen alloys which showed marked improvement of fatigue life when hydride particles were present, while fatigue crack propagation rates were not significantly affected. It was noted that stress-assisted hydrides formed only in the originally hydrided alloys and that their formation enhanced fatigue resistance.

The work on delayed failure was initiated to determine the role of hydrogen in solution and/or as a hydride phase in vanadium alloys on the delayed failure and notched fatigue characteristics.

EXPERIMENTAL PROCEDURE

Two different shapes of vanadium (99.8% purity) have been obtained from Wah Chang Corp.; rod form for notched fatigue tests and sheet form for delayed failure studies. The rod specimens, originally in the cold-worked condition, were annealed for one hour at 1050°C in vacuum, then furnace cooled. The sheet samples of vanadium were received in the annealed condition, and were annealed as described in Part 1. Both forms of specimen were then annealed for 2 hours at 760°C in vacuum to give final grain sizes of 85 μ m. Hydrogen gas was in contact with the specimens

for two hours at 600°C for rods and at 660°C for sheets respectively, followed by slow cooling to room temperature. For fatigue tests three levels of H₂ were introduced: ~ 132, 400, and 1000 ppm, corresponding to contents in earlier unnotched fatigue tests.⁵ For delayed failure tests (stress-rupture) four levels of hydrogen were introduced: 200, 430, 845, and 1500 ppm, corresponding to contents used in earlier work propagation studies, see Table 1.

Fully reversed tension-compression fatigue tests in stress-control mode were conducted at room temperature by applying a sine wave at 20 Hz on a closed-loop electrohydraulic machine; these test conditions are similar to those utilized for the previous unnotched fatigue studies.⁵ For delayed failure tests, specimens were dead-weight loaded at room temperature in a creep-rupture testing machine and times to rupture were recorded at various load levels. The theoretical stress concentration factor (K_t) was determined from Peterson¹⁷ and found to be 10.2 for the rod specimens and 5.8 for the sheet specimens respectively.

RESULTS

Delayed Failure

Results of delayed failure experiments on unalloyed vanadium and the hydrogenated alloys are shown in Fig. 4. It appears that vanadium and its solid-solution alloys with hydrogen are nearly insensitive to delayed failure, indicating non-embrittlement characteristics. Examination of fracture surfaces revealed significant amounts of plastic flow and necking prior to fracture. Hydrided alloys, however, show typical features of delayed failure, analogous to those observed in other materials which exhibit delayed failure in hydrogen. For example, an incubation time

for crack initiation was noted, followed by a period of slow crack propagation. An application of a nominal stress intensity, $K_1 = 8.4 \text{ MN} \cdot \text{m}^{-3/2}$ for 260 hours in a hydrided alloy (845 ppm H_2) resulted in a significant amount of hydride reorientation and growth at the root of the notch, see Fig. 5. The hydride plates are reoriented normal to the applied stress axis. Fig. 5 reveals early crack initiation at the root of the notch in the region of stress-induced hydride growth; it shows that the initial crack is transgranular, parallel to the reoriented hydride platelets. In order to observe crack propagation behavior, the hydrided alloy (845 ppm H_2) was precracked by cyclic loading and then slowly cracked under sustained load; the appearance of the initial cracks was similar in both conditions, but significant amounts of hydride grew only in the delayed failure specimen. This indicates that the formation of stress-assisted hydrides can be more effectively accomplished under the sustained load condition than under cyclic loading. Insignificant secondary cracking was noted at the interface of hydride and matrix, which is quite contrary to observations made on Nb and other alloys.³ Metallographic examination of 430 ppm H_2 alloys below the solubility limit of hydrogen in vanadium) revealed no formation of stress-induced hydride in both delayed failure and fatigue failure tests, although extensive plastic deformation occurred at the root of the notch.

Fracture surfaces of annealed vanadium and 200 ppm H_2 alloys could not be examined fractographically due to chisel point fractures which involved excessive plastic deformation at the point of fracture. The 430 ppm H_2 alloy fractured with some combination of shear and cleavage regions. The fracture surfaces of the 845 and 1500 ppm H_2 alloys exhibited only the cleavage mode in all stress intensity ranges.

Fatigue Notch Sensitivity

Fig. 6 is a plot of stress amplitude (σ) vs. number of cycles (N) for several notched vanadium-hydrogen alloys. In comparison to previously reported data for unnotched vanadium,⁵ there is little influence of notches on the σ -N curve. A striking difference in behavior of vanadium-hydrogen alloys was noted, however. While notched samples showed a sharp drop in fatigue life with increasing hydrogen content, particularly rapid for 130 ppm material, hydrogen at all levels increased the lives of unnotched samples. Fig. 6 shows little difference in endurance limit between the 400 ppm H_2 and 1000 ppm H_2 alloys, unlike the results for unnotched alloys.

Fracture modes in notched specimens were essentially similar to those observed in ref. 5; annealed vanadium revealed ductile striations. Wavy striations were also seen in 200 ppm H_2 alloys, but were interspersed with regions of cleavage in the 400 ppm H_2 alloy. V-1000 ppm H_2 showed only cleavage facets.

DISCUSSION

The stress intensities for unstable fracture, K_M , and the threshold stress intensities, K_{TH} , as a function of hydrogen content in vanadium, obtained from Fig. 4, are summarized in Fig. 7, together with the schematic lines for the estimation of the delineation between non-embrittlement and embrittlement failure conditions at room temperature. K_{TH} in the present tests was defined as the highest initial stress intensity to a given specimen with $K_t = 5.8$ which could be loaded without anticipation of failure within 1000 hours. It should, however, be noted that these values are of comparative use only, being strongly dependent upon the K_t value. Both K_{TH} and K_M values decreased with increasing hydrogen concentration,

corresponding to increasing yield stresses, see Table 1. This trend may be explained on the basis of the local variation of stress concentration factors at notch roots in the alloys. The yield strength can only effectively provide limiting stress values for the maximum values of stress which can be attained at the root of notch, and thus plastic deformation at the root of a notch will lower the stress concentration factor. This indicates that for a given applied stress intensity in the range of small plastic deformation, the stress concentration factor should be greater as the yield strength increases, simply because there will be less plastic flow in the critical zone. The results also demonstrate that the alloys containing hydrogen in solution deform in a normal manner, with no significant effect of stress on the rupture time. This result should be considered in conjunction with the observation that alloys with hydrogen in solution did not form stress-induced hydrides regardless of the applied stress levels, consistent with results of high cycle fatigue crack propagation tests, see Part 1.

The effects of hydrogen on the notched fatigue endurance limit, σ_e , at 10^7 cycles, obtained from Fig. 6, and notch sensitivity factor, $q = K_f^{-1}/K_{t-1}$, are summarized in Fig. 8. The fatigue strength reduction factor, K_f , defined as endurance limit in absence of a notch, divided by endurance limit in notched condition, and theoretical concentration factor, K_t , are shown in Table 5. Alloys containing a high hydrogen content (i.e. 1000 ppm H_2) have high notch sensitivity, leading to poor fatigue properties, compared to the marked improvements in properties noted in smooth specimens. In addition, it can be seen that as hydrogen is increased, the fatigue notch sensitivity factor, q , and strength reduction factor, K_f , (see Table 5) more nearly approach the values expected from

theoretical stress concentration factors. This indicates that the stress gradient produced in the specimen by a notch results in an appreciable decrease in stress at the notch root with decreasing hydrogen content. Consequently, for the same peak stress, 1000 ppm H₂ specimens are subject to the most severe stress gradient in a region located in the critical zone established by the notch.

Part 3

EFFECTS OF TEST FREQUENCY ON FATIGUE OF V-H₂ ALLOYSINTRODUCTION

Previous work in our laboratory has shown that hydrides increase the room temperature stress-controlled fatigue resistance of polycrystalline vanadium⁵ and that the effect may be related to both delayed crack initiation and slowed crack propagation under identical crack tip stress conditions. The earlier work showed also that σ -N curves obtained by plotting saturation stresses in strain-controlled tests vs. number of cycles to failure did not agree well with σ -N curves for stress-control experiments in the case of hydrided alloys only.⁵ This anomalous behavior has previously been noted for molybdenum,¹⁸ and has been attributed to the increased frequency usually employed in stress-controlled experiments. The present work is concerned with frequency effects on fatigue life of vanadium-hydrogen alloys.

EXPERIMENTAL PROCEDURE

Vanadium was obtained and heat treated as described previously.⁵ Fatigue and tensile experiments were conducted on specimens with 1 cm long gage length and 0.5 cm gage diameter. All samples were electropolished prior to testing to remove machine marks. Fully reversed tension-compression fatigue tests were conducted in either stress or strain control in a closed-loop electrohydraulic machine. For stress-controlled tests at 25°C, 20 Hz and 1 Hz frequencies were employed, with a sinusoidal wave shape. Strain-controlled tests were run with a triangular wave to maintain a constant strain rate; frequency ranged from 0.2 to 1 Hz, depending upon the maximum strain imposed. Cyclic hardening data were monitored with an

X-Y recorder.

RESULTS

Fatigue Tests

The effects of test frequency are shown in Fig. 9a) for vanadium and 9b) for V-1000 ppm H_2 , together with strain control data run at a frequency near 1 Hz. The strain control data were obtained by plotting saturation stresses vs. number of cycles to failure. The cyclic strain hardening data obtained in these tests have previously been reported.⁵ It is clear that reducing test frequency from 20 Hz to 1 Hz lowers the entire σ -N curve and that data for 1 Hz tests agree reasonably well with strain control data.

Observation of Crack Paths

Surface deformation markings obtained from 1 Hz stress control tests were almost the same as those observed from strain control tests. Slip band cracking and intergranular-transgranular crack growth were noted for annealed vanadium, and transgranular cleavage cracks initiating at hydride plates were observed for the V-1000 ppm H_2 alloy.

DISCUSSION

The discontinuity in the σ /N curves obtained from stress-control and strain-control tests in molybdenum has previously been attributed to time dependent dislocation multiplication which is dependent upon the test frequency.¹⁸ Fig. 9 shows that there is indeed a small test frequency effect on high cycle life of vanadium, which appears to be responsible for the small discontinuity in the σ /N curves obtained by stress and strain control. The reduction in fatigue limit due to the decrease in the test

frequency is not as great as for molybdenum.¹⁸ The ratio of FL/UTS is about 0.52, higher than usually noted for fcc metals. Since the same high ratio of FL/UTS is obtained at two frequencies differing by a factor of 20, and strain aging is very sensitive to strain rate, the effects of strain aging on fatigue limit seems to be minimal in this material. Therefore, the high ratio of FL/UTS is probably an inherent property of vanadium and other bcc metals, due perhaps to the high ratio of elastic limit to ultimate tensile strength, coupled with a low monotonic hardening rate.

The pronounced effect of test frequency on fatigue life of hydrided vanadium, Fig. 9b), is related to its dislocation structure; dislocation multiplication is more time dependent than for annealed vanadium, probably due to interaction between the mobile dislocations and geometrically necessary ones on the precipitate interfaces. A decrease in the initial cyclic hardening rate of hydrided vanadium compared to annealed vanadium⁵ also indicates that dislocation motion or multiplication was hindered by the hydride plates. A significant decrease in fatigue lifetimes with decreasing frequency has previously been noted for low-carbon steels¹⁹ and polycrystalline α iron.²⁰ In the latter investigation fatigue crack initiation was shown to depend sensitively on strain rate. Consequently, it may be assumed that the increased flow stress in bcc metals at higher strain rates delays crack initiation, particularly in two phase materials or single phase materials in which strain aging may occur.

Part 4

FATIGUE OF NIOBIUM-HYDROGEN ALLOYS

INTRODUCTION

The present work extends the investigation of influence of hydrogen on fatigue behavior of group Va metals to unalloyed niobium, two niobium-hydrogen solid solution alloys and two hydrided alloys. Fatigue experiments have been conducted under both strain and stress control at room temperature and have been correlated with hydrogen-induced cyclic hardening behavior and fracture morphology.

EXPERIMENTAL PROCEDURE

Niobium received from Wah Chang Corp. (99.9% purity) was in the form of annealed rod (1.27 cm diam.) with a grain size of $\sim 100 \mu\text{m}$. Fatigue and tensile test specimen with 1.0 cm gage length and 0.56 cm gage diameter were first machined from the as-received niobium and then mechanically polished. An annealing treatment was conducted at 700°C for 2 hours in a vacuum of 10^{-7} torr, resulting in a final grain size of $110 \mu\text{m}$. Hydrogen was added by the same technique as for vanadium⁵ for two hours at 660°C ; the specimens were then furnace cooled. Chemical analyses and microstructures of niobium and the niobium alloys are shown in Table 6. Solid solution alloys with 110 and 270 ppm hydrogen, as well as hydrided alloys with 750 and 1180 ppm hydrogen were obtained. Tensile tests were conducted at room temperature in air with a strain rate of $5 \times 10^{-3} \text{ min}^{-1}$. Stress-controlled fatigue tests were conducted in a closed-loop electrohydraulic machine, at a frequency of 20 Hz, at room temperature in air. Strain-controlled tests were performed with a triangular wave to maintain a constant strain rate; test frequencies

ranged between 0.2 and 1 Hz, depending upon maximum strain. Cyclic hardening was monitored during constant strain tests by a X-Y recorder. These test procedures were identical to those employed in the earlier work on V-H₂ alloys.⁵

EXPERIMENTAL RESULTS

Tensile Tests

The tensile behavior of niobium-hydrogen alloys tested at room temperature is summarized in Table 7. The 0.2% offset yield stress of niobium was increased substantially with increasing hydrogen content but a severe reduction of ductility with hydrogen content resulted in only limited improvement of ultimate tensile strength. Similar tensile data for niobium-hydrogen alloys have been reported in the literature.

Fracture modes were dimpled rupture (chisel point fracture) in annealed niobium and cleavage in the hydrogen charged alloys. Both alloy conditions, either with hydrogen in solution or as hydride precipitates, revealed numerous cracks in the early stages of plastic deformation. The general surface cracking morphologies in tension were similar to those observed in vanadium.

Fatigue Tests

Fig. 10 shows the results of stress-controlled cycling tests in niobium with various levels of hydrogen in the form of σ , applied stress, vs. N_f , number of cycles to failure. It shows that fatigue life of niobium improves with increasing hydrogen content; the fatigue limits, σ_e , at 10^7 cycles are appreciably increased in the hydrided alloys, although only small increments in fatigue life were noted at higher applied stresses. The ratios of σ/σ_{UTS} as a function of N_f , plotted in Fig. 11, seem to fall into a single line at higher stress levels

and deviate at lower stress levels. The values of the ratios of σ_e / σ_{UTS} at 10^7 cycles are in the range of 0.5-0.7 generally reported for bcc metals.

Strain-controlled fatigue tests were conducted with the same materials used in stress control. The results are analyzed in terms of total strain $\Delta\epsilon_t / 2$ against N_f , as plotted in Fig. 12. The fatigue life of annealed niobium is not significantly affected by changing cyclic mode from stress control to strain control and reducing test frequency, but fatigue lives of the hydrogenated alloys in strain control are progressively reduced with increasing hydrogen content. These poor fatigue lives of the present alloys in strain control are similar to the observation made in the hydrogenated vanadium alloys,⁵ which may in part be accounted for by the deleterious effects of reduced cyclic frequency.

Fracture Morphology

Fracture surfaces of annealed niobium samples consisted mainly of ductile striations. No significant differences in fracture mode between stress control and strain control were observed in annealed niobium. However, the 110 ppm H₂ alloy shows a mixed mode of cleavage-striation failure in stress control, but mainly cleavage facets in strain control. Both test conditions led to significant amounts of plastic flow combined with fibrous features and river lines on the fracture surface. Crack propagation in stress-control tests on the 110 ppm H₂ alloy seemed to be effectuated primarily through the formation of wide, shallow striations on the cleavage plane, while in strain control cracking is associated with a complicated cleavage mechanism. Fracture surfaces (stress control) of 270 ppm H₂ alloy were basically similar to those of the 110 ppm H₂ alloy (striations formed on cleavage planes perpendicular to river lines), but

secondary cracks often formed along cleavage steps, and this seems a typical mode of mixed shear-cleavage failure. In contrast, strain control tests on 270 ppm H₂ alloys resulted mainly in larger flat cleavage facets and also a significant number of grain boundary cracks, although failure processes were mainly transgranular.

The fracture surfaces of hydrided niobium alloys in stress control consisted of highly faceted cleavage surfaces, with a small amount of secondary cracking, and occasionally intergranular cracks followed by extensive cleavage steps on a small scale. Strain control, on the other hand, resulted in large cleavage facets with grain boundary secondary cracks, which are similar to those observed in the 270 ppm H₂ alloy in strain control.

Surface morphologies observed by conventional metallographic techniques were generally consistent with features on the fractographs: alloys with hydrogen in solution at low stresses revealed an insignificant amount of secondary surface cracking but at higher stresses multiple secondary cracks parallel to the primary crack were observed. Hydrided alloys exhibited mainly large secondary cracks at the interface between matrix and hydride phase while the primary crack followed a mixed intergranular-transgranular path.

DISCUSSION

The results reported here are preliminary, but seem to indicate the same general effects of hydrogen on fatigue life of niobium and vanadium. Detailed analysis of the data must await determination of cyclic strain hardening data, observations of crack initiation and propagation, and determination of the effect of hydrogen on the dislocation

substructure generated by fatigue of niobium.

OVERALL SUMMARY

The room temperature cyclic behavior of vanadium-hydrogen alloys has been shown to depend sensitively upon both microstructural and external test conditions. Preliminary work to date on niobium-hydrogen alloys has revealed a pattern of behavior in high and low cycle fatigue of unnotched samples similar to that observed for vanadium. The following is a summary of the most important results and conclusions of our work:

1. Hydrogen in solution has a small beneficial influence on fatigue behavior of unnotched vanadium and niobium tested in the high cycle range.
2. Hydrides produce a marked improvement in fatigue life of both unnotched vanadium and niobium tested in the high cycle range.
3. Hydrogen at all levels is detrimental to low cycle fatigue resistance of vanadium and niobium. Hydrides are particularly harmful.
4. Test frequency is an important variable for hydrided vanadium.
5. Hydrides delay crack initiation and early propagation in unnotched vanadium; crack propagation rates are increased by hydrogen for the same test conditions. Crack propagation rates depend upon the cyclic strain hardening rate, n' , and the yield stress. For identical crack tip plastic zone sizes, hydrides slow crack propagation.
6. The detrimental effects of hydrides on low cycle fatigue behavior arise from three conditions:
 - a) decreased fatigue resistance at the low test frequencies characteristic of low cycle tests

- b) decreased monotonic tensile ductility
- c) decreased cyclic strain hardening rates.

7. The introduction of a sharp notch into unalloyed vanadium has little effect, but causes a pronounced deterioration in fatigue properties of hydrogenated alloys. The notch sensitivity index increases with hydrogen content.

8. Hydrided vanadium is subject to delayed failure; unalloyed vanadium and solid solution vanadium-hydrogen alloys do not exhibit delayed failure.

9. Pre-existing vanadium hydrides grow and reorient in the triaxial stress field ahead of a notch or crack. No hydrides are observed as a result of stressing solid solution vanadium-hydrogen alloys.

10. Fatigue striations are noted in unalloyed niobium, but increasing hydrogen content lead to a cleavage mechanism of crack growth.

ADDITIONAL CONTRACT INFORMATION

Effort and Compliance

The principal investigator, N. S. Stoloff, has been devoting approximately 25% time during the academic year, except for the four months period 1 September, 1976 - 1 January, 1977, when he was on sabbatical leave and no time was charged to the program. Effort during the summer months was at 1/3 time. For the balance of the current contract year 35% time will be charged to the contract in view of extensive efforts in preparing several papers for publication. The 25% academic year, 1/3 time summer months level of effort is planned for the period 5/1/77 - 4/30/78. Dr. D. W. Chung, a post-doctoral research associate, has been working full-time on this program. K. S. Lee received his Ph.D. degree in Fall, 1976. R. Venkateshwar was employed

as a research assistant during the Fall 1976 semester, but was recently withdrawn from Rensselaer. An undergraduate research assistant will be employed to assist Dr. Chung.

The essential tasks outlined in Proposal No. 175(76R)B308(21) which formed the basis for the research reported here have been complied with as of this date.

Reports and Publications

COO 3459-8 "Effect of Oxygen on Deformation and Fracture of Polycrystalline Oxygen", by R. L. Straw and N. S. Stoloff, was published in Metallurgical Transactions, V. 7A, 1976, pp. 312-314.

COO 3459-9 "Fatigue of Vanadium-Hydrogen Alloys", by K. S. Lee and N. S. Stoloff, was published in Proc. Conf. on Effect of Hydrogen on Behavior of Materials, AIME, New York, 1976, pp. 404-414.

A paper entitled "Effect of Hydrogen on Fatigue Crack Propagation in Vanadium", by D. W. Chung and N. S. Stoloff has been submitted to Metallurgical Transactions.

A paper entitled "Effects of Temperature and Test Frequency on Fatigue of V-H₂ Alloys", by K. S. Lee and N. S. Stoloff, is to be submitted for publication during February 1977.

A paper entitled "Delayed Failure and Fatigue Notch Sensitivity of Vanadium-Hydrogen Alloys", by D. W. Chung and N. S. Stoloff, is to be submitted for publication during February 1977.

REFERENCES

1. C. W. Owen, D. H. Sherman and T. E. Scott, Trans. Met. Soc. AIME, 1967, vol. 239, p. 1666.
2. D. G. Westlake, Trans. Met. Soc. AIME, 1969, vol. 245, p. 1969.
3. H. K. Birnbaum, M. Grossbeck and S. Gahr, "Hydrogen in Metals", I. M. Bernstein and A. W. Thompson, Eds., Amer. Soc. for Metals, 1974, vol. 2, p. 303.
4. B. A. Wilcox, Trans. Met. Soc. AIME, 1964, vol. 230, p. 1199.
5. K. S. Lee and N. S. Stoloff, "Effect of Hydrogen on Behavior of Materials", AIME, New York, 1976, p. 404. See also Annual Report, Contract E(11-1)-3459, COO 3459-10, Jan. 15, 1976.
6. W. F. Brown, Jr. and J. E. Srawley, ASTM STP 410, Am. Soc. Test. Mat., 1969, p. 10.
7. P. C. Paris, Paper 62-MET-3 ASME, Amer. Soc. Mech. Eng., New York, 1962.
8. P. C. Paris and F. Erdogan, J. Basic Eng., ASME, 1963, vol. 85, p. 528.
9. R. O. Ritchie and J. F. Knott, Acta Met., 1973, vol. 21, p. 639.
10. S. M. El-Soudani and R. M. Pelloux, Met. Trans., 1973, vol. 4, p. 519.
11. J. P. Hickerson and R. W. Hertzberg, Met. Trans., 1972, vol. 3, p. 179.
12. R. W. Hertzberg, Met. Trans., 1974, vol. 5, p. 306.
13. B. Tomkins, Phil. Mag., 1968, vol. 18, p. 1041.
14. F. A. McClintock and R. M. Pelloux, Document Dl-81-0708, Boeing Scientific Res. Lab, Seattle, 1968, p. 1.
15. J. Weertman, Proc. 1st Conf. Fract., Sendai, Japan, 1966, vol. 1, p. 153.

16. J. R. Rice, ASTM STP 415, Amer. Soc. for Test Mat., Philadelphia, 1967, p. 247.
17. R. E. Peterson, "Stress Concentration Design Factors", John Wiley & Sons, New York, N.Y., 1953, p. 16.
18. P. Beardmore and P. H. Thornton, Met. Trans., 1970, vol. 1, p. 775.
19. D. E. Gucer and M. Capa, Met. Trans., 1970, vol. 1, p. 3075.
20. H. Mugrabi, Z. Metallk., 1975, vol. 66, p. 719.

Table 1
Chemical Analysis of Vanadium Alloys and Their Yield Stresses

<u>Specimens</u>	<u>H</u>	<u>O</u>	<u>N</u>	<u>Yield Stress</u> (MN/m ²)	<u>Microstructure</u>
	(in ppm)				
V-Annealed	6	65	27	136.5	Solid Solution
V-H200	200	--	--	146.1	Solid Solution
V-H420	420	170	39	173.3 ⁴	Solid Solution
V-H520	520	130	12	181.7	Hydride (20 μ m)
V-H845	845	190	43	189.3	Hydride (40 μ m)
V-H1000	1000	300	--	192.5	Hydride (60 μ m)
V-H1500	1500	480	57	203.7 ⁴	Hydride (70 μ m)

Table 2

Fatigue Crack Propagation Data for Vanadium and Hydrogen Charged Vanadium Alloys at Various Stress Range and Mean Stress Ratios.

<u>Specimens</u>	<u>$\Delta\sigma$ (MN/m²)</u>	<u>R (= $\frac{\Delta K_{min}}{\Delta K_{max}}$)</u>	<u>\bar{m}</u>	<u>C (cm/cycle)</u>
V-Annealed	46.06	0.4	2.63	3.67×10^{-9}
V-H200	43.92	0.4	3.0	3.05×10^{-9}
V-H420	44.68	0.4	6.99	1.97×10^{-9}
V-H1500	43.99	0.4	7.7	2.80×10^{-11}
V-H420	43.92	0.05	6.5	3.35×10^{-11}
V-H520	43.44	0.05	7.15	5.18×10^{-11}
V-H830	43.85	0.05	6.7	3.68×10^{-11}
V-H1500	43.37	0.05	7.7	2.48×10^{-11}
V-H420	43.92	0.05	6.5	3.35×10^{-11}
V-H420	44.82	0.4	6.99	1.97×10^{-9}
V-H420	31.37	0.516	8.33	9.44×10^{-11}
V-H1500	32.27	0.05	7.7	2.79×10^{-11}
V-H1500	32.27	0.516	8.7	2.39×10^{-11}
V-H1500	43.92	0.05	7.7	2.48×10^{-11}
V-H1500	43.99	0.4	7.9	1.89×10^{-11}

Table 3

Data for Power Law Exponent, m , in Fatigue Crack Propagation Equation, Compared in Fatigue Strain Hardening Exponent, n' .⁵

<u>Specimen</u>	<u>m</u>	<u>n'</u>	<u>$m' (m'/n' = m)$</u>
V-Annealed	2.63 *	0.33	0.872
V-H200	3.00 *	0.297	0.892
V-H420	6.5	0.159	1.032
V-H520	7.15	0.1 **	0.715
V-H830	6.70	0.1 **	0.67
V-H1500	7.70	0.08	0.61

* $R = 0.4$

** Approximated from a plot of n' vs. σ_y/σ_{UTS}

Table 4

Data for Fatigue Crack Growth Rate Constant, C, in Paris Equation in Comparison with Yield Stresses, σ_y , in Vanadium Alloys

Specimen	<u>C</u> (cm/cycle)	<u>σ_y (MN/m²)</u>	<u>$\alpha (\alpha/\sigma_y^2 = C) (m^{1/2})$</u>
V-Annealed	3.67×10^{-9}	136.5	6.8×10^{-5}
V-H200	3.05×10^{-9}	146.1	6.5×10^{-5}
V-H420	1.97×10^{-9}	173.3	5.9×10^{-5}
V-H520	* 5.18×10^{-11}	181.7	1.7×10^{-6}
V-H830	* 3.68×10^{-11}	189.3	1.3×10^{-6}
V-H1500	2.79×10^{-11}	203.7	1.2×10^{-6}

* R = 0.05

Table 5

Fatigue Notch Sensitivity Data in Vanadium-Hydrogen Alloys

<u>Specimen</u>	<u>K_t</u>	<u>K_f</u>	$q = \frac{K_f - 1}{K_t - 1}$ at 10^7 cycles
V-Annealed	10.2	1.44	0.156
V-H200	10.2	2.35	0.255
V-H400	10.2	4.14	0.45
V-H1000	10.2	6.98	0.652

Table 6
Chemical Analyses of Niobium-Hydrogen Alloys

<u>Alloys</u>	<u>H</u>	<u>O</u>	<u>N</u>	<u>Microstructures</u>
			(in ppm)	
Nb-Annealed	2	112	21	solid solution
Nb-H110	110	-	-	solid solution
Nb-H270	270	290	31	solid solution
Nb-H750	750	340	34	hydride phase
Nb-H1180	1180	320	64	hydride phase

Table 7
Tensile Data for Niobium-Hydrogen Alloys

<u>Alloys</u>	<u>0.2% σ_y</u> (MN/m ²)	<u>UTS</u> (MN/m ²)	<u>Uniform ϵ (%)</u>	<u>Total ϵ (%)</u>
Nb-Annealed	103.307	182.126	35	90 (45)
Nb-H110	118.150	213.417	31	40.5
Nb-H270	121.136	223.340	32	41
Nb-H750	127.091	217.35	18	26
Nb-H1180	153.373	223.595	14.5	21

FIGURE CAPTIONS

1. Fatigue crack propagation rates, da/dN , plotted as a function of stress intensity factor, ΔK , at room temperature for various hydrogen concentrations in vanadium.
2. Fatigue crack propagation rates, da/dN , vs. stress intensity factor, ΔK , at mean stress ratio, $R = 0.05$, in hydrogen charged vanadium alloys.
3. Number of cycles, ΔN_i , (to initiate a crack length of $\Delta C \approx 0.0127$ cm) against hydrogen concentration in vanadium alloys at applied stress range $\Delta \sigma = 87.7 \text{ MN/m}^2$.
4. Stress intensity vs. time to failure in vanadium-hydrogen alloys.
5. Stress-induced hydride at the root of a notch in 845 ppm H_2 alloy, loaded to $K_1 = 8.4 \text{ MN}\cdot\text{m}^{-3/2}$ for 260 hours at room temperature.
6. Stress amplitude vs. number of cycles to failure for hydrogen alloys:
 - a) notched, b) unnotched.
7. Stress intensity for unstable fracture and threshold stress intensity as a function of hydrogen concentration in vanadium, showing the boundary of delayed failure mode between alloys with hydrogen in solution and hydrided alloys.
8. Fatigue notch sensitivity factor and endurance limit as a function of hydrogen content in vanadium-hydrogen alloys.
9. Effect of test frequency on fatigue of a) vanadium and b) V-1000 ppm H_2 .
10. Stress amplitude vs. cycles to failure of niobium and niobium-hydrogen alloys.
11. $\sigma/\sigma_{\text{UTS}} - N_f$ plot for niobium and niobium-hydrogen alloys.
12. Total strain amplitude against cycles to failure of niobium and niobium-hydrogen alloy.

Fig. 1. Fatigue crack propagation rates, da/dN , plotted as a function of stress intensity factor, K , at room temperature for various hydrogen concentrations in vanadium.

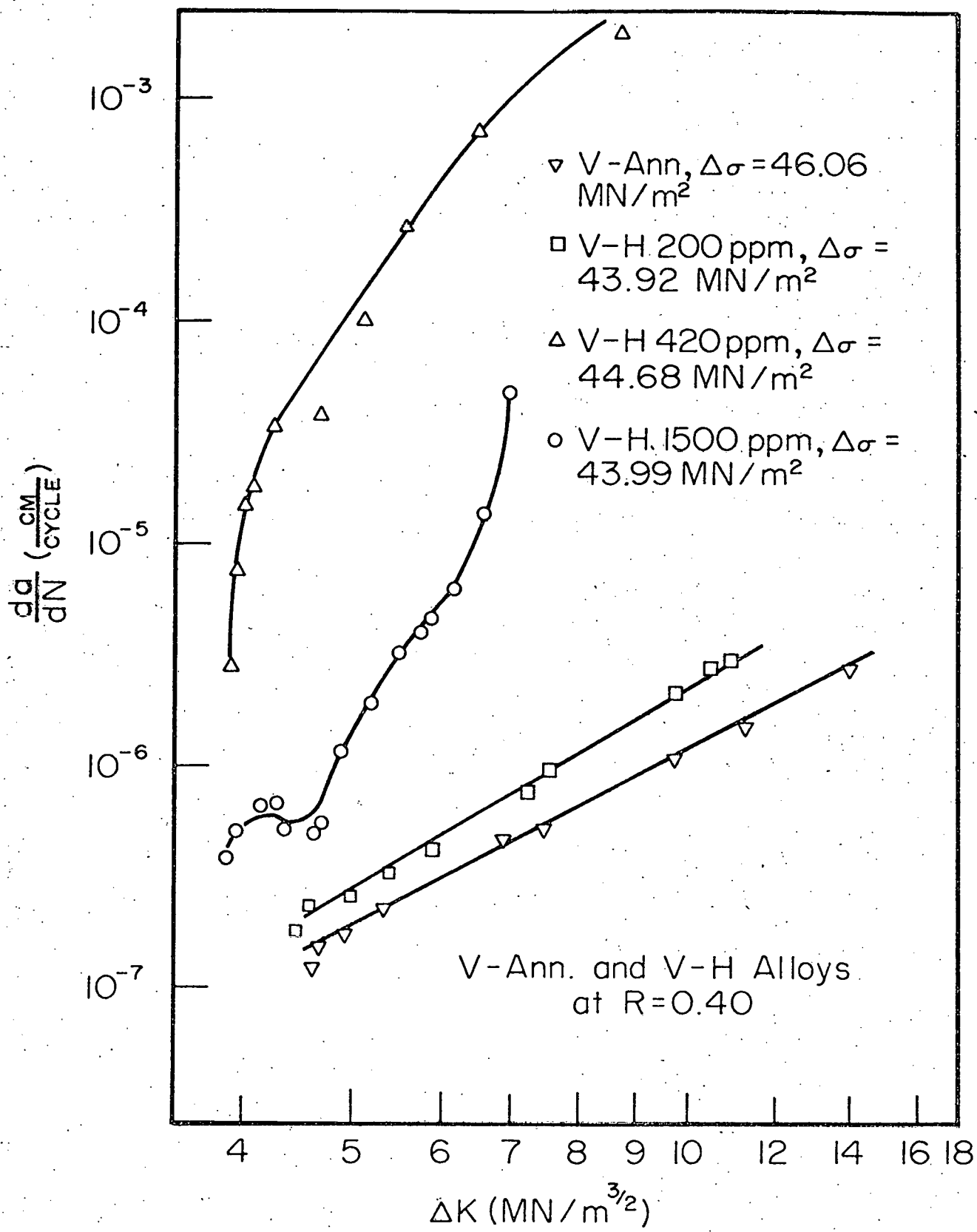


Fig. 2. Fatigue crack propagation rates, da/dN , vs. stress intensity factor, K , at mean stress ratio, $R = 0.05$, in hydrogen charged vanadium alloys.

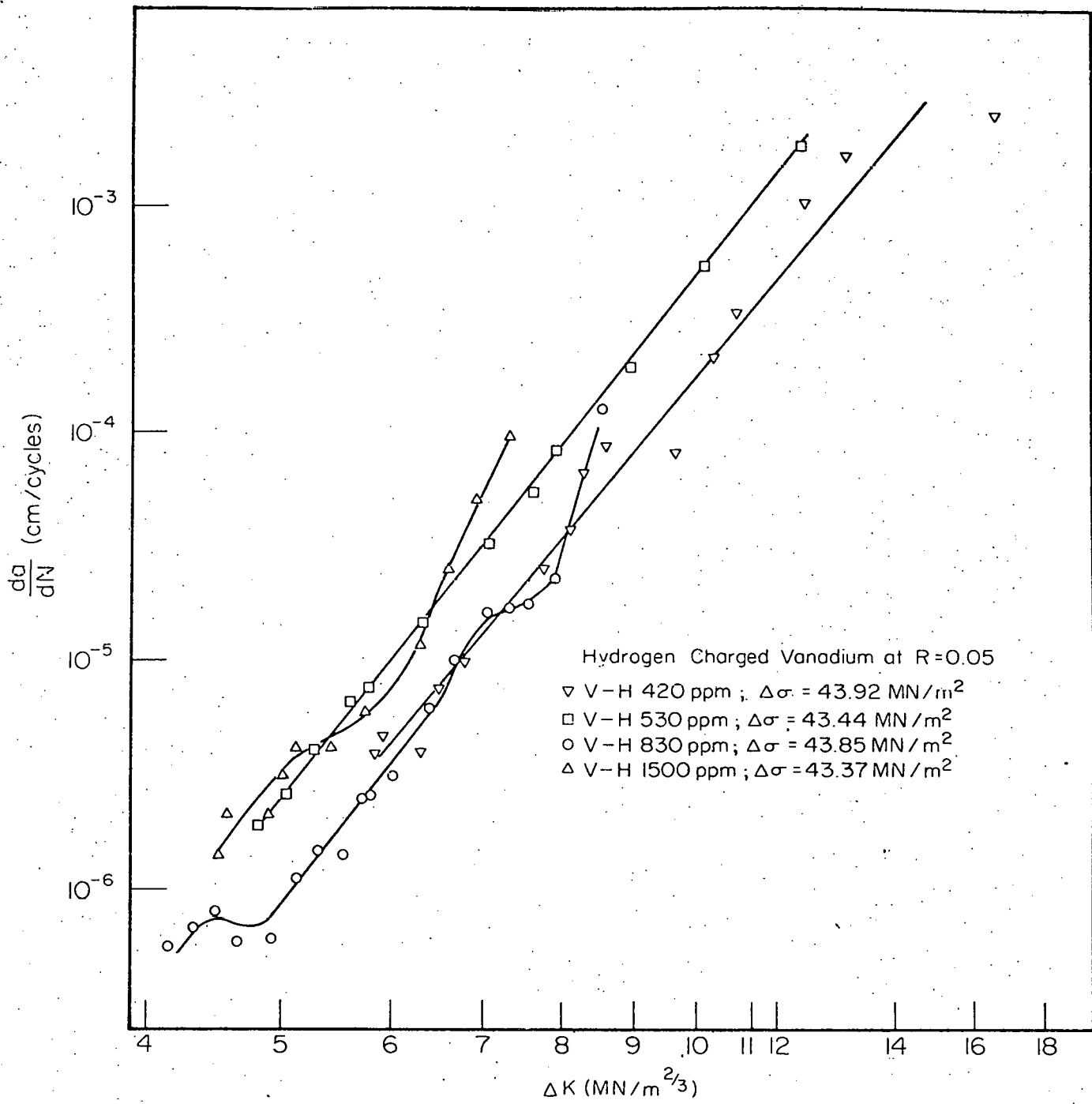
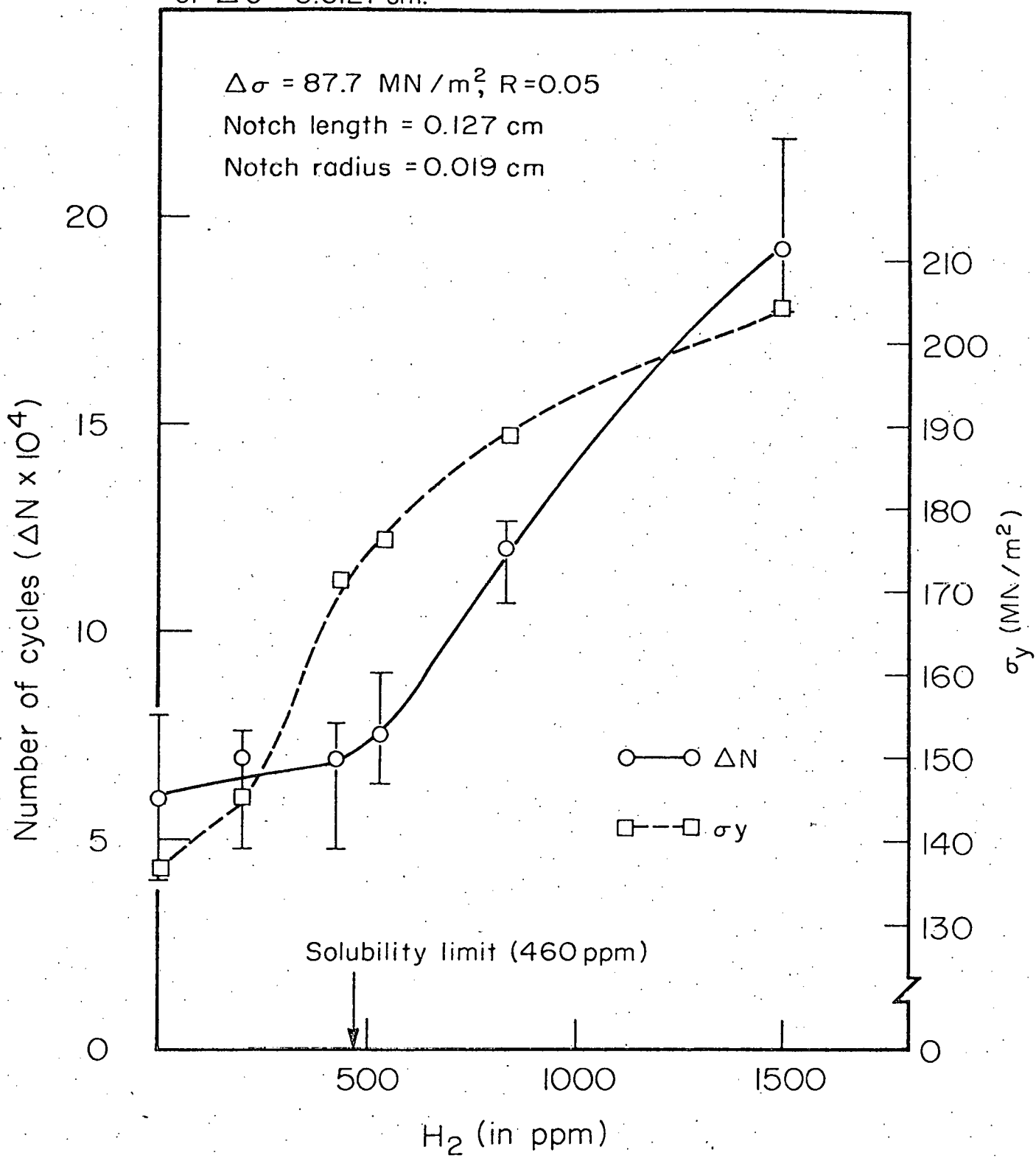


Fig. 3. Number of cycles, ΔN_i , (to initiate a crack length of $\Delta C \approx 0.0127$ cm) against hydrogen concentration in vanadium alloys at applied stress range, $\Delta\sigma = 87.7$ MN/m².

Number of Cycles for the Initiation of the Crack Length
of $\Delta C \approx 0.0127$ cm.



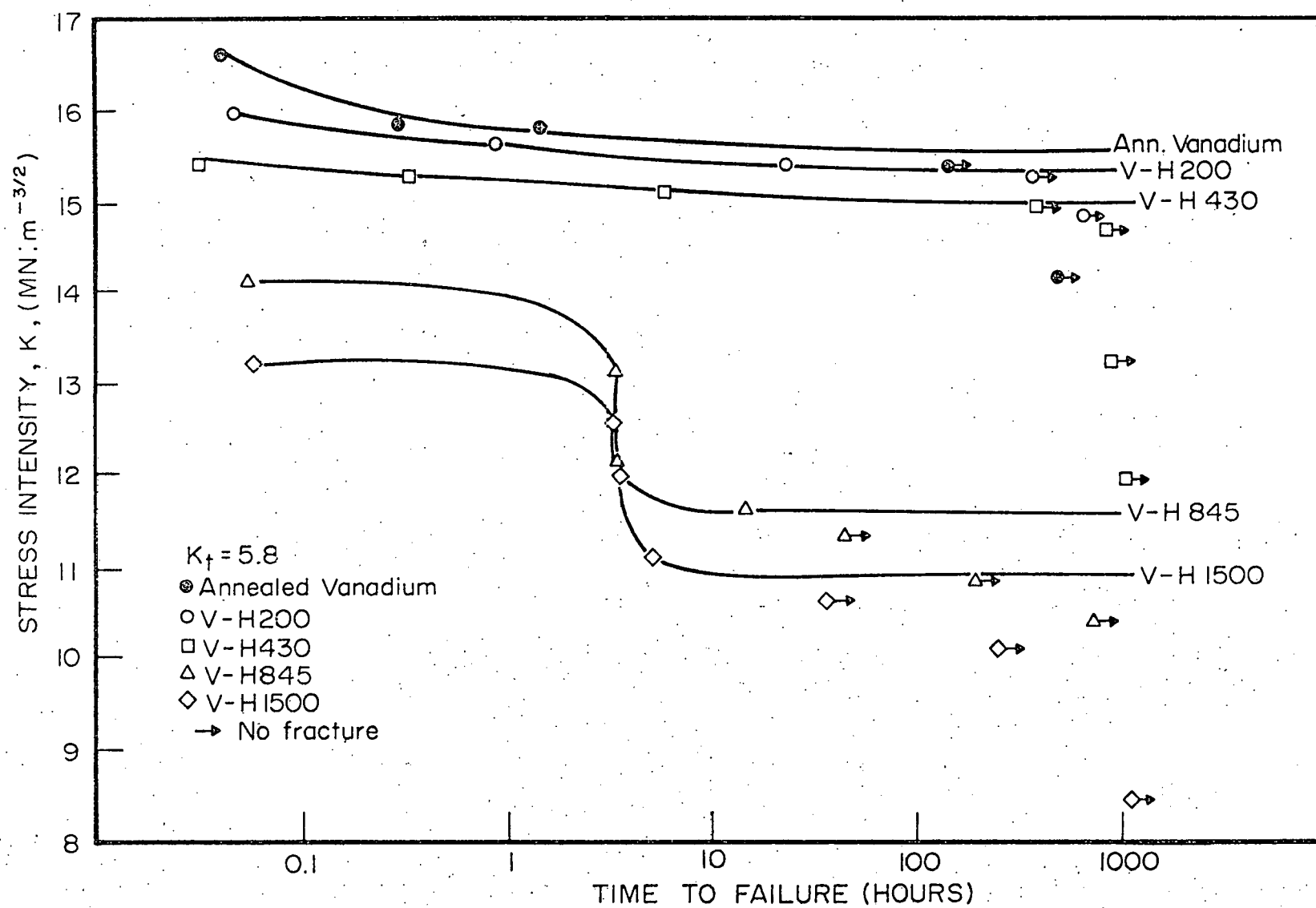


Fig. 4. Stress intensity vs. time to failure in vanadium-hydrogen alloys.



Fig. 5. Stress-induced hydride at the root of a notch in 845 ppm H₂ alloy, loaded to $K_1 = 8.4 \text{ MN}\cdot\text{m}^{-3/2}$ for 260 hours at room temperature.

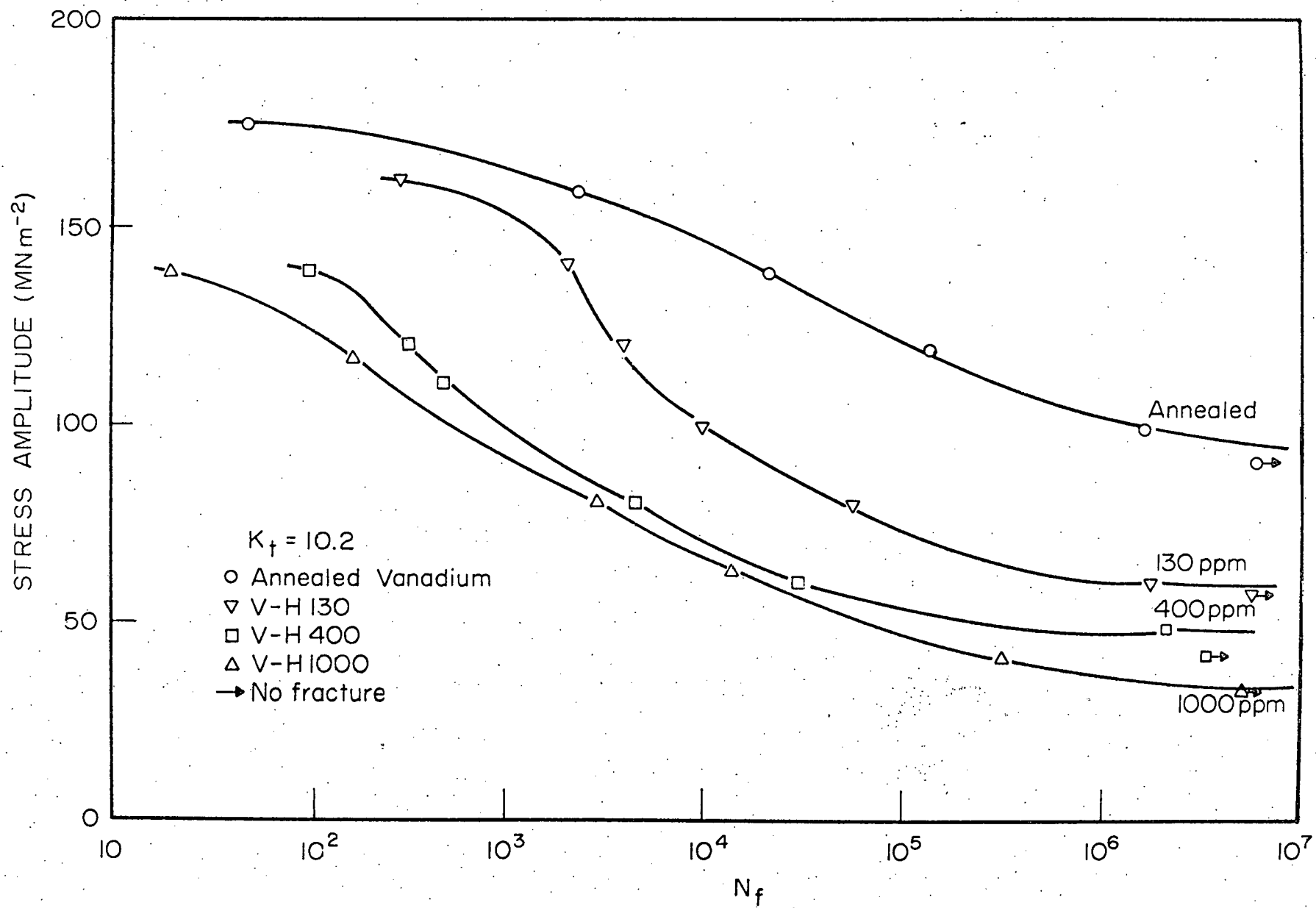


Fig. 6. Stress amplitude vs. number of cycles to failure for hydrogen alloys: a) notched, b) unnotched.

Fig. 7. Stress intensity for unstable fracture and threshold stress intensity as a function of hydrogen concentration in vanadium, showing the boundary of delayed failure mode between alloys with hydrogen in solution and hydrided alloys.

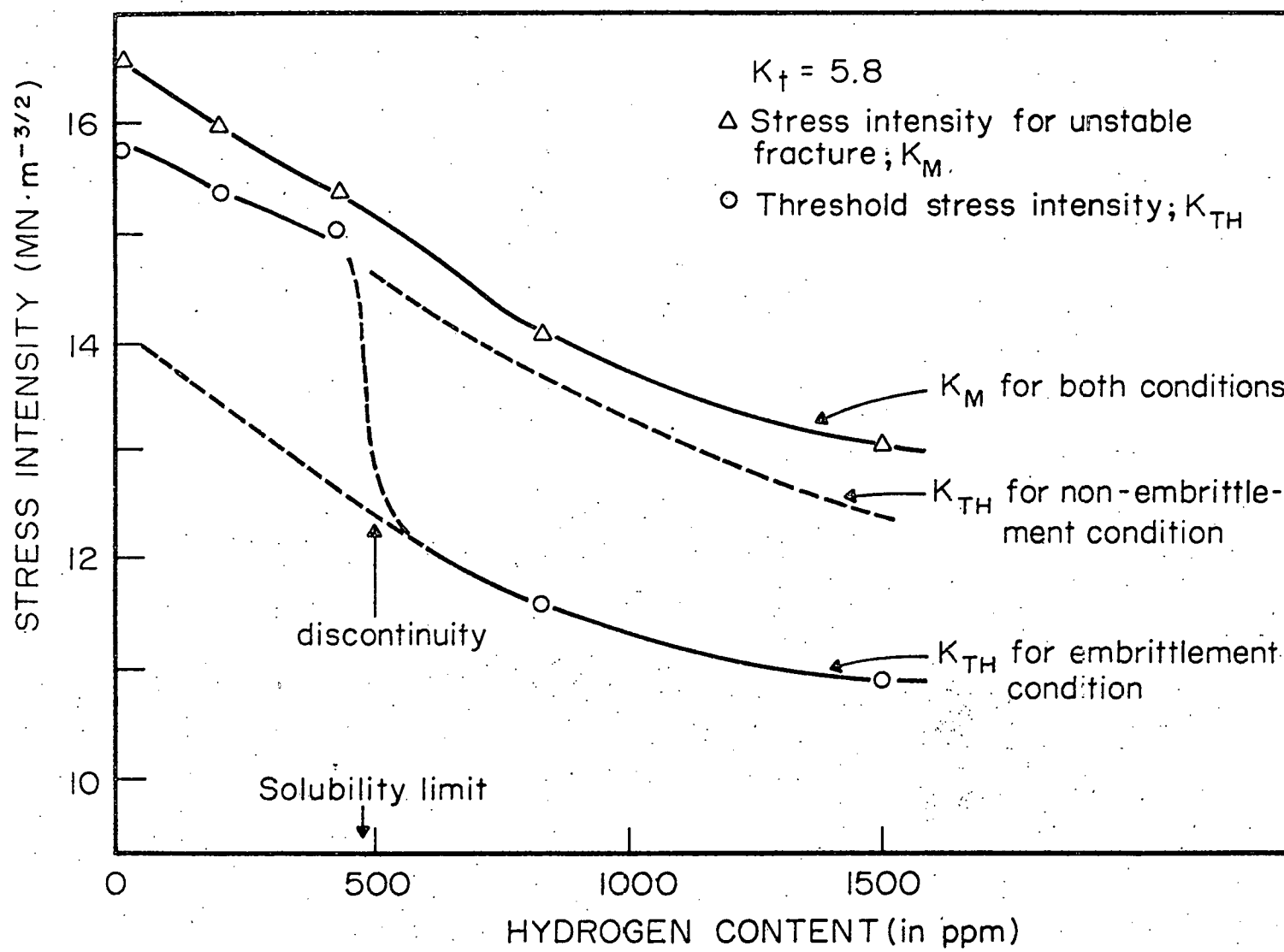


Fig. 8. Fatigue notch sensitivity factor and endurance limit as a function of hydrogen content in vanadium-hydrogen alloys.

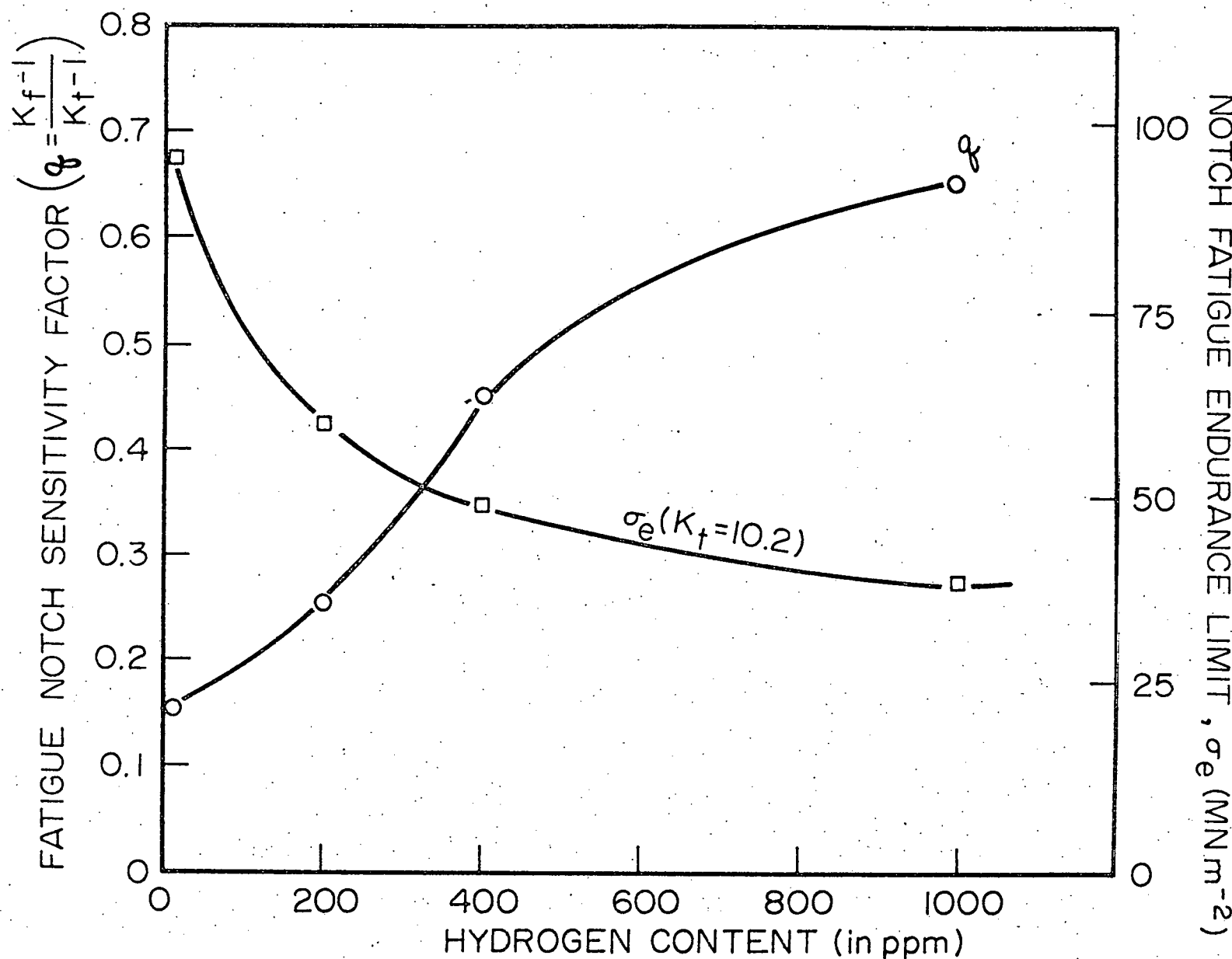


Fig. 9(a)

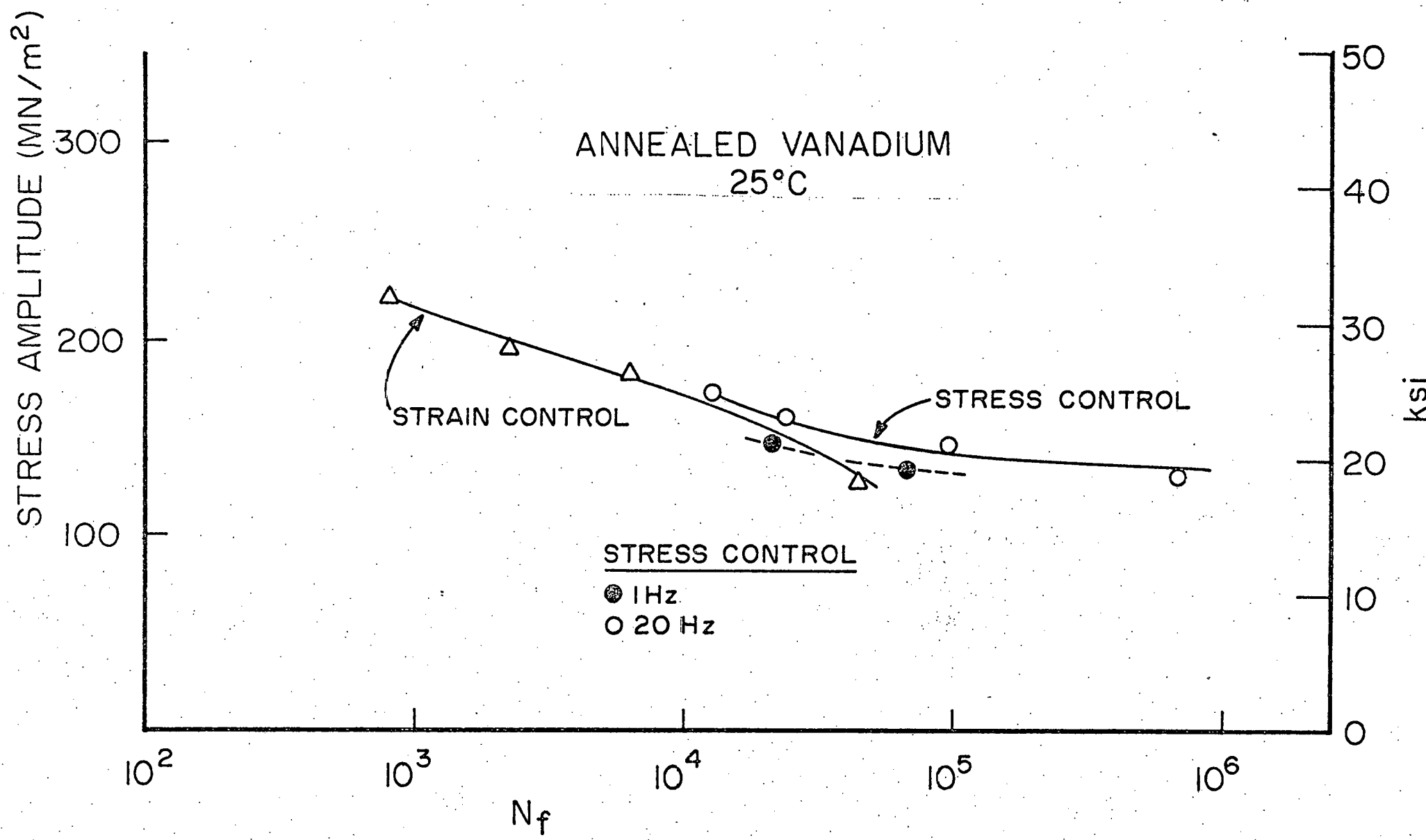


Fig. 9(b)

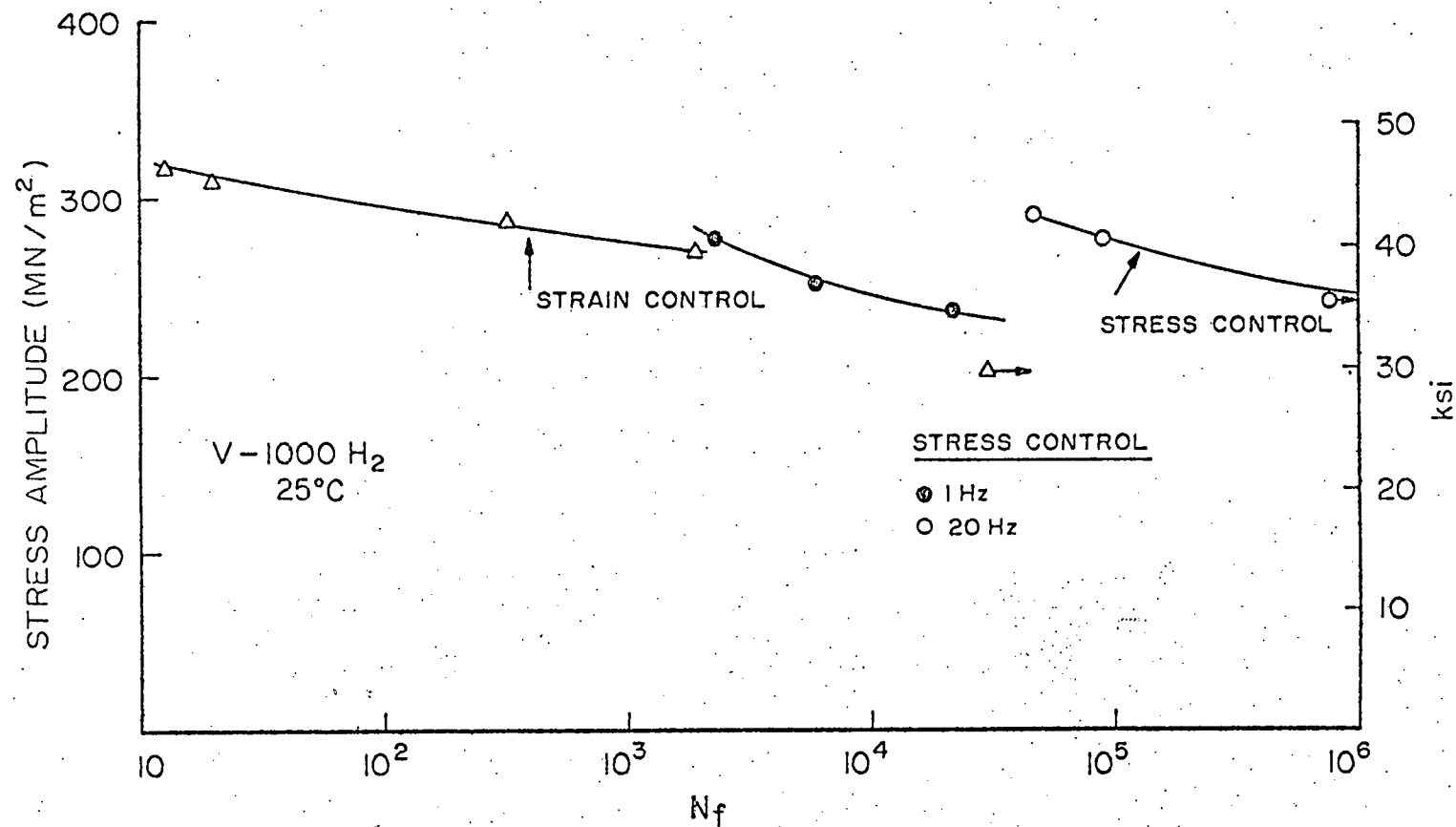


Fig. 9. Effect of test frequency on fatigue of a) vanadium and
b) V-1000 ppm H₂.

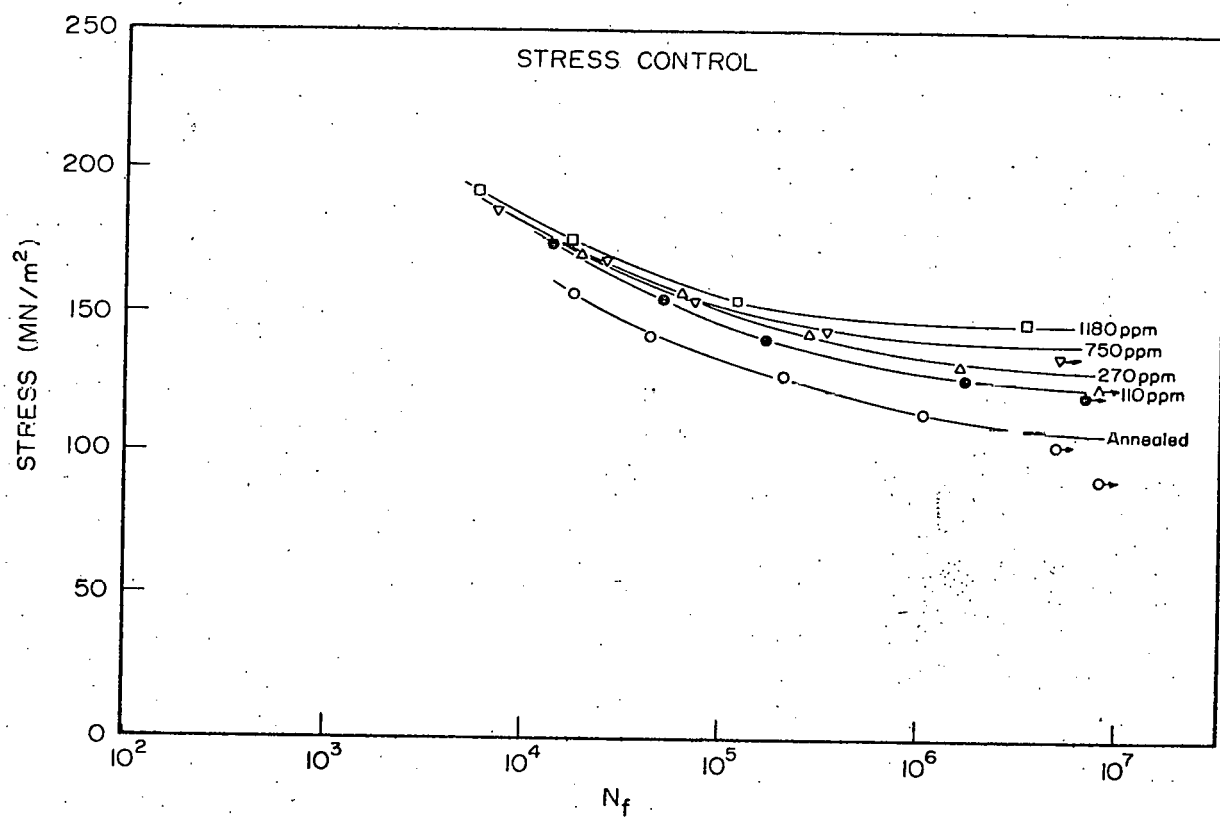


Fig. 10. Stress amplitude vs. cycles to failure of niobium and niobium-hydrogen alloys.

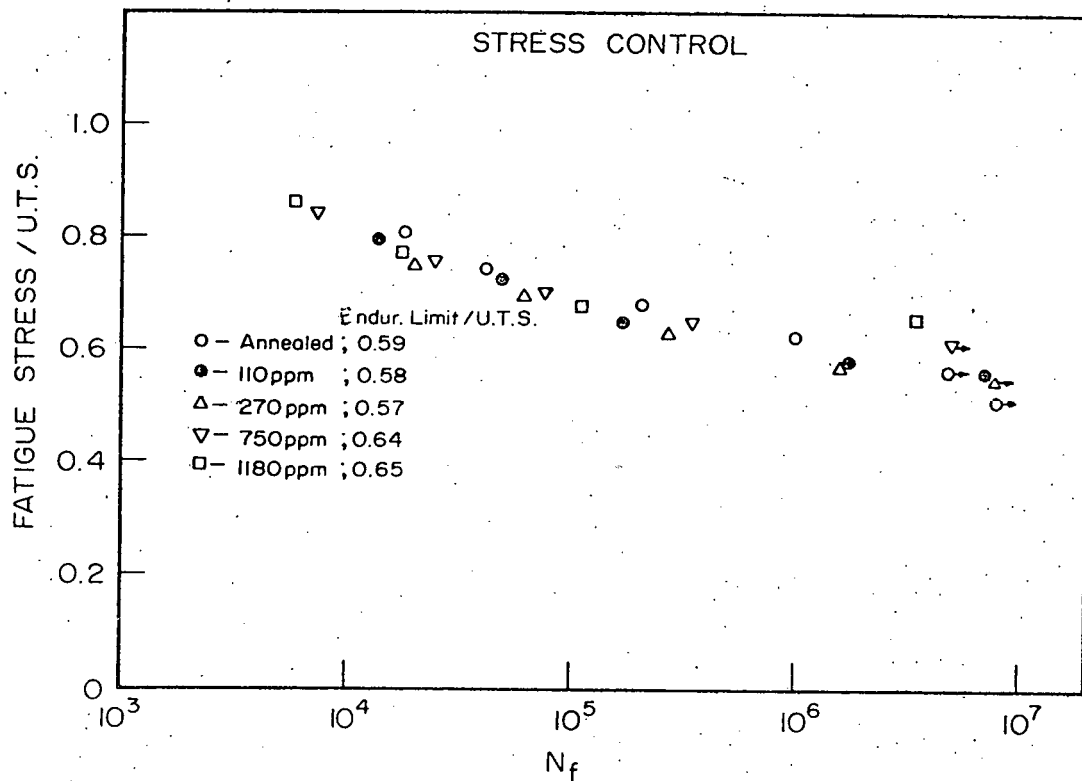


Fig. 11. σ/σ_{UTS} - N_f plot for niobium and niobium-hydrogen alloys.

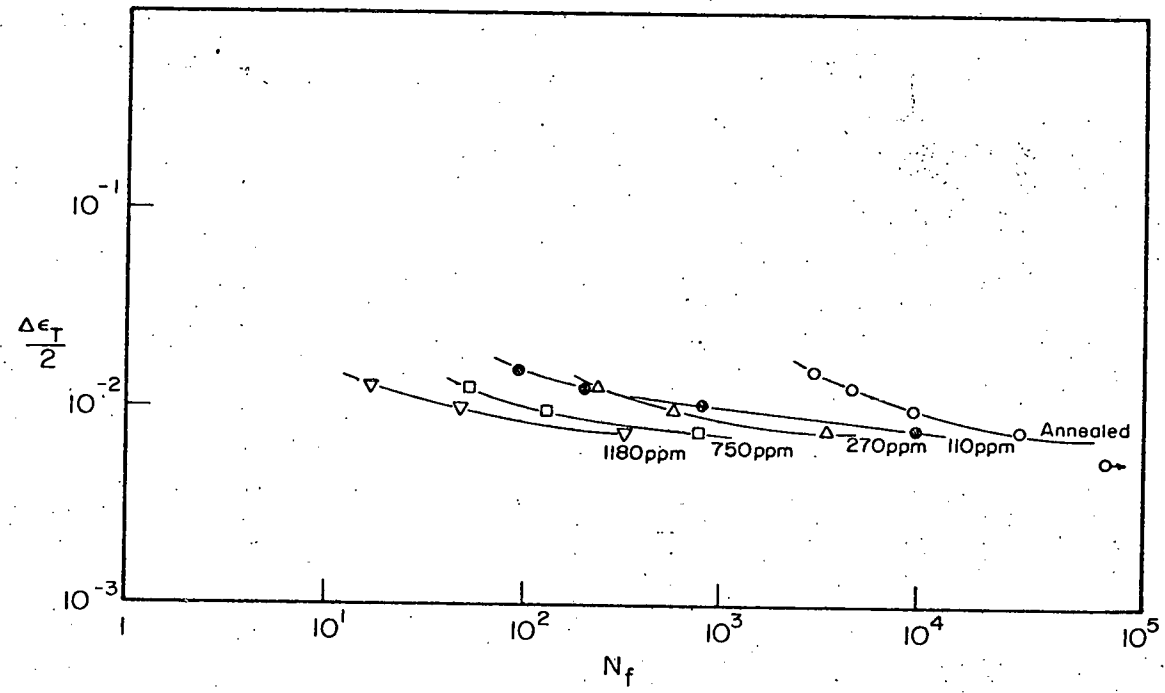


Fig. 12. Total strain amplitude against cycles to failure of niobium and niobium-hydrogen alloys.